Quantitative Solids Mixing Analysis Using Interpretable Image Processing Methods

Ansony Rolando Medina Baca[1], Abdelmalik Moujahid[1*†], Javier Sánchez-Prieto[1†], Kiet Tran-Trung[2†]

[1*] Universidad Internacional de la Rioja, Av. de la Paz, Logroño, 26006, La Rioja, Spain.
[2] Ho Chi Minh City Open University, Ho Chi Minh, 35-37, Vietnam.

*Corresponding author(s). E-mail(s): abdelmalik.moujahid@unir.net; Contributing authors: ansonyrolando.medina-externo@unir.net; javier.sanchez.prieto@unir.net; kiet.tt@ou.edu.vn;
†These authors contributed equally to this work.

Abstract

This study presents a quantitative framework for evaluating lateral mixing in a bubbling fluidized bed based on high-speed image analysis and Lacey mixing index estimation. Experiments were conducted in a pseudo-two-dimensional fluidized bed using optically distinguishable glass beads, enabling detailed tracking of mixing dynamics over time. Recorded images were processed through a pipeline comprising contrast enhancement, noise reduction, and segmentation via adaptive thresholding to isolate tracer particles. Spatial concentration fields were then extracted from the segmented images and used to estimate local variances necessary for computing the Lacey index as a time-resolved measure of mixing progression from a fully segregated to a randomly mixed state.

By providing clear, quantitative indicators of mixing evolution, the proposed methodology offers a potential basis for integrating interpretable measurements into digital models of fluidized bed systems. These image-based insights could contribute to improving the transparency of digital representations of fluidized beds and support future efforts toward explainable digital twins for process monitoring and control. The results suggest that combining classical image processing with statistical metrics provides a reliable means to analyze and understand complex mixing dynamics in a way that may be incorporated into interpretable digital frameworks.

Keywords: Image processing, Fluidized beds, Solid mixing, Statistical mixing metrics

1 Introduction

Gas-solid fluidized beds are widely utilized across numerous industrial sectors, including chemical manufacturing, pharmaceuticals, energy, and food processing, due to their superior gas-solid contact and heat transfer capabilities. The operational effectiveness of these systems largely depends on achieving and maintaining homogeneous solid-phase mixing, as inadequate mixing can induce localized temperature and concentration gradients that detrimentally affect process efficiency and product quality [1]. In particular, the solid mixing rate in thermochemical energy conversion processes determines the location and design of fuel feeding ports in fluidized bed boilers [2].

The hydrodynamics of fluidized beds, characterized by bubble formation, coalescence, and eruption, coupled with complex gas-solid interactions, govern the mixing mechanisms of particulate solids [3]. The axial component of solid mixing is known to be induced by bubble rising, while the lateral dispersion of solid mixing is promoted by bubble coalescence and eruption [4]. Belgardt et al. [5] confirmed that the axial mixing component is much faster than the lateral mixing, allowing the use of one-dimensional Fickian-type diffusion model for the estimation of lateral dispersion coefficient, which has been extensivelly used on the quantification of solid mixing on fluidized beds.

Traditional experimental solid mixing quantification methods primarily rely on tracer studies and physical sampling, which, despite their reliability, are often intrusive and limited in temporal resolution [6, 7]. Optical imaging techniques, on the other hand, enable non-invasive, high-temporal-resolution observations of mixing dynamics, especially effective in pseudo-2D fluidized beds where direct particle visualization is feasible [8–10]. These techniques also provide the information needed to determine the mixing time and the mixing curves relaying on mixing index [11], instead of estimating the lateral dispersion coefficient. However, the extraction of quantitative mixing metrics from image data is challenged by factors such as particle overlap, illumination variability, and the inherent projection of three-dimensional distributions onto two-dimensional planes [3, 12].

The mixing phenomena in fluidized beds has been also studied by means of numerical simulation models, such as two-fluid model (TFM) [13–15] and discrete element model (DEM) [16, 17]. While continuum-based numerical frameworks, such as TFM, have advanced the understanding of fluidized bed behavior through detailed simulations [13, 18], experimental validation remains essential to capture the intrinsic complexities and validate modeling assumptions. Techniques like Particle Image Velocimetry (PIV) and visual tracking in pseudo-two-dimensional fluidized beds provide valuable experimental insights [19].

In this context, the present work proposes a robust quantitative framework for evaluating lateral mixing in a bubbling fluidized bed by integrating classical image processing techniques with statistical mixing metrics. The experimental system employs optically distinguishable glass beads arranged initially in a laterally segregated configuration and fluidized by air. High-speed imaging captures the evolving spatial distributions of the particle phases, which are processed through a pipeline of contrast enhancement, noise reduction, and segmentation to isolate tracer particles.

From the processed images, spatial concentration fields are constructed and used to compute the Lacey mixing index, a normalized statistical measure that quantitatively tracks the transition from segregation to random mixing [20]. This approach reveals distinct mixing stages, including an initial convective transport phase induced by bubble dynamics followed by a slower diffusive redistribution. The resulting temporal evolution of the mixing index enables the extraction of characteristic mixing times and lateral dispersion coefficients, offering a quantitative description of the mixing process.

By demonstrating that classical image analysis methods combined with appropriate statistical indices can effectively characterize dynamic particulate flow behavior, this study contributes an experimentally validated tool for analyzing fluidized bed mixing. The proposed methodology complements existing modeling efforts [4, 21, 22] and supports the experimental validation of numerical simulations [2, 23], thereby facilitating improved process optimization and control.

2 Experimental Setup

The experimental facility consists of a pseudo-two-dimensional cold fluidized bed designed to study mixing dynamics through image-based analysis. A schematic representation of the setup is shown in Fig. 1, adapted from [11].

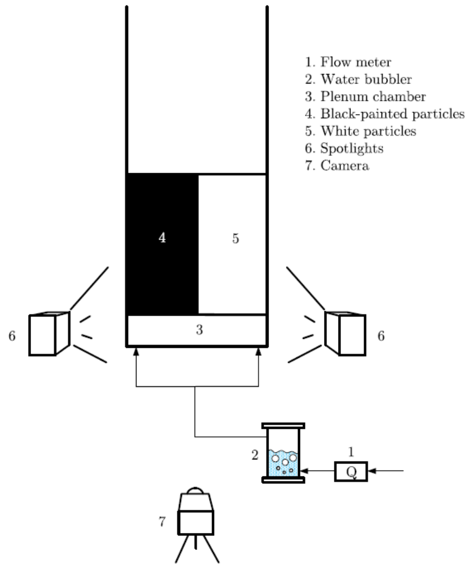

Fig. 1: Schematic diagram of the experimental setup. Adapted from [11].

- **Airflow System:** The gas supply is controlled using a flow meter (1) and a water bubbler (2), ensuring a constant and measurable air flow. This air passes through a plenum chamber (3) which distributes the fluidizing gas uniformly across the bed's base. The plenum chamber is equipped with a perforated plate with two rows of 30 holes of 1 mm diameter arranged in a triangular configuration with 1 cm pitch.

It provides the pressure drop needed to avoid gas maldistribution [24] the bubble formation in the bed and prevents the falling of particles inside the plenum chamber.

- **Fluidized Bed:** The main column of the bed has internal dimensions of 0.3 m (width) $\times$ 1 m (height) $\times$ 0.01 m (thickness), thus it can be considered a pseudo-2D fluidized bed. The bed is initially loaded with ballotini glass particles (2500 kg/m^3 density) and particle size of 0.4–0.6 mm. To visually distinguish phases during analysis, half of the particles are painted in black (4), while the remaining unpainted particles appear white (5). The painting process does not affect the physical properties of the particles, as was demonstrated by [11] using Scanning Electron Microscopy (SEM) images.
- **Lighting and Imaging:** Two spotlights (6) were symmetrically placed at the front to ensure uniform illumination of the bed and minimize shadows or lighting gradients. A Nikon digital camera (7), positioned perpendicular to the bed's front wall, captures video at 60 frames per second with a spatial resolution of 1280 $\times$ 720 pixels. Each pixel corresponds to an approximate physical dimension of 0.4 mm, which defines the spatial resolution limit for identifying features in the mixing process.
- **Mixing Procedure:** Prior to each experiment, a vertical partition is inserted along the bed's centerline to form two symmetric compartments. The left side is filled with black particles and the right side with white particles, yielding a completelly segregated state at the beginning of each experiment. Once filled, the partition is removed, and the air flow is initiated at a controlled superficial velocity. This sudden activation initiates the mixing process, which is recorded for post-processing and image-based quantification.

The mixing process in fluidized beds can be defined as the transition from the completely segregated state, where particles of different colours (e.g. black and white) are fully separated laterally within the bed, to a randomly mixed state characterized by an apparently uniform spatial distribution of particles without preferential patterns. The completely unmixed state corresponds to the maximum lateral segregation, where one type of particle occupies one side of the bed and the other type occupies the opposite side. Conversely, the randomly mixed state is achieved when particles are distributed such that any random sample taken from the bed reflects the overall particle proportions, indicating homogeneity at the system level.

To quantitatively assess the mixing quality, the states of the granular mixture are represented through probability distributions of particle locations. These distributions are then condensed into scalar mixing indices, which serve as objective metrics to track the degree of mixing over time. This approach enables the characterization of mixing dynamics from image data by transforming spatial information into meaningful numerical indicators.

3 Image-Based Estimation of Mixing Quality

In this study, image analysis is employed to evaluate the evolution of mixing in a pseudo-2D fluidized bed system. The core metric used to quantify the degree of mixing is the *Lacey index*, which provides a normalized measure of mixing quality based on spatial variance in particle concentrations. To ensure the robustness of the computed index, images recorded during the mixing process are preprocessed through a sequence of classical enhancement and segmentation steps prior to quantitative analysis.

The digital video recordings, acquired at 60 frames per second and with a spatial resolution of 1280×720 pixels, are first subjected to noise and artifact removal. This step includes the application of Gaussian filtering, where the kernel width σ is selected to attenuate high-frequency noise while preserving the structural integrity of particle edges [25]. Following this preprocessing, each frame is converted from a color image to a grayscale intensity image to provide a consistent basis for subsequent analysis.

The enhanced grayscale image is then segmented by clustering the pixel intensities into three distinct classes, producing a labeled map that assigns each pixel to one of three categories: class 1 (background), class 2 (black solid phase), or class 3 (white solid phase). This segmentation delineates the different phases or components present within the mixture captured in the image.

From the segmentation map, binary masks are generated separately for class 2 and class 3, indicating the spatial distribution of each of these two phases in the image domain. The image is partitioned into non-overlapping tiles of fixed size, and within each tile, the local concentration of a given class is calculated as the fraction of pixels in the tile assigned to that class.

The variance of the local concentration distribution across all tiles is then computed for each class, serving as a measure of the spatial heterogeneity of the corresponding phase. The variance in the completely segregated state, denoted σ_0^2, is defined as

$$\sigma_0^2 = \bar{c}\,(1 - \bar{c})\,,$$

where $\bar{c}$ represents the mean concentration of the class in the entire image. The variance expected at the randomly mixed state, denoted σ_R^2, is given by

$$\sigma_R^2 = \frac{\sigma_0^2}{n},$$

where n corresponds to the total number of tiles in which the image is divided.

The Lacey Mixing Index for each class is subsequently calculated using the expression

$$M = \frac{\sigma_0^2 - \sigma^2}{\sigma_0^2 - \sigma_R^2},$$

where σ^2 is the measured variance of local concentrations for the class under consideration. The Lacy index usually has a zero value for the completely segregated state and increases to unity for the randomly mixed state, following an exponential trend [20].

This calculation is applied independently to the binary masks of class 2 and class 3, yielding two separate indices that quantify the homogeneity of each phase. In addition, a global mixing index for the entire image can be determined by evaluating the combined distribution of the three classes, providing a comprehensive measure of the overall degree of mixing.

Repeating this procedure across all frames of the video sequence enables the construction of time series of the Lacey Mixing Index, facilitating a quantitative analysis of the temporal evolution of mixing dynamics.

4 Numerical Results

In this section, we present the numerical analysis of the mixing process based on image segmentation and the computation of the Lacey mixing index. The segmentation procedure is applied to a representative frame to classify pixels into distinct phases within the flow field, enabling precise spatial characterization of the mixture. This segmentation discriminates between background and phases of interest, forming the basis for further quantitative analysis.

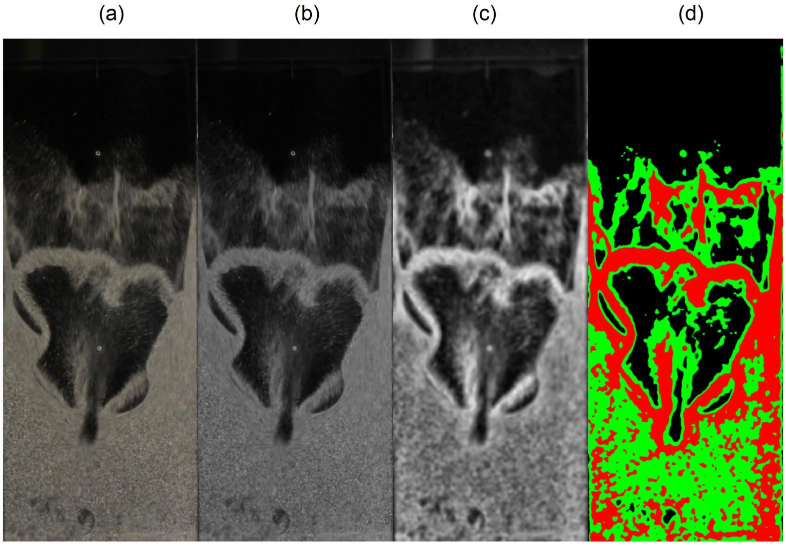

Fig. 2: Segmentation procedure for a representative frame. (a) Original RGB image, (b) Grayscale converted image, (c) Gaussian filtered image for noise reduction, (d) Final segmented map with three classes: background (black), class 2 (green), and class 3 (red).

Figure 2 illustrates the segmentation procedure applied to a representative frame of the experimental data. The original RGB image (a) is first converted to a grayscale intensity image (b), which is then filtered to reduce noise while preserving relevant structural features. The final segmentation map (d) classifies the image into three classes: background (black), class 2 (green), and class 3 (red). This segmentation provides the foundation for phase identification and further quantitative analysis.

To provide additional perspective on the spatial distribution of each solid phase, Figure 3 shows an overlay of the local concentration map onto the corresponding grayscale image of one segmented phase. The image is subdivided into a grid of tiles, and within each tile, the local concentration is estimated as the fraction of pixels belonging to the phase. This local concentration is represented by a red intensity overlay, with higher intensities indicating relatively greater phase presence.

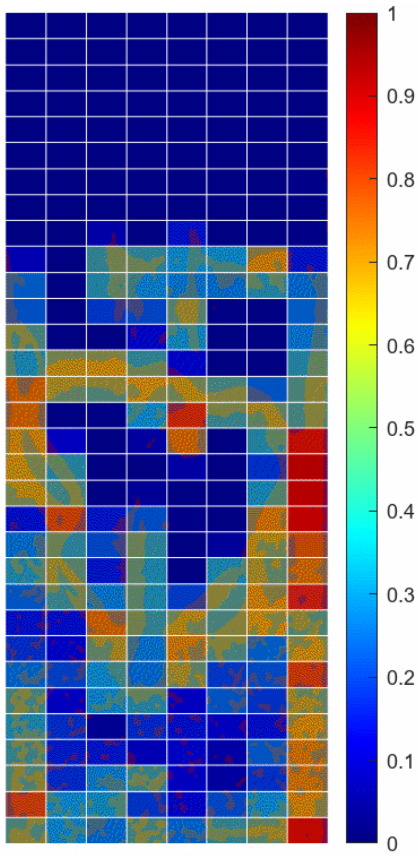

Fig. 3: Visualization of the local concentration map overlaid on the grayscale image of a segmented phase. The red overlay indicates the estimated local concentration in each tile, highlighting regions of higher and lower phase concentration. This facilitates qualitative assessment of spatial uniformity and mixing progression.

This visualization offers a qualitative view of spatial variations in phase distribution, which may assist in interpreting patterns of homogeneity and segregation within the sample. While it does not provide a definitive quantitative measure on its own, the overlay can support the assessment of mixing characteristics and highlight areas that warrant further analysis. Such an approach complements the computed mixing indices by providing spatial context that may be relevant in understanding the mixing process.

Finally. the temporal evolution of the mixing process is evaluated by calculating the Lacey mixing index for the two solid phases identified through segmentation. The segmentation classifies the images into three classes: background, solid phase 1 (black particles), and solid phase 2 (white particles). Figure 4 shows the Lacey index for each solid phase over time, reflecting changes in spatial homogeneity during the mixing process. This analysis provides an indication of the mixing progression for each phase independently.

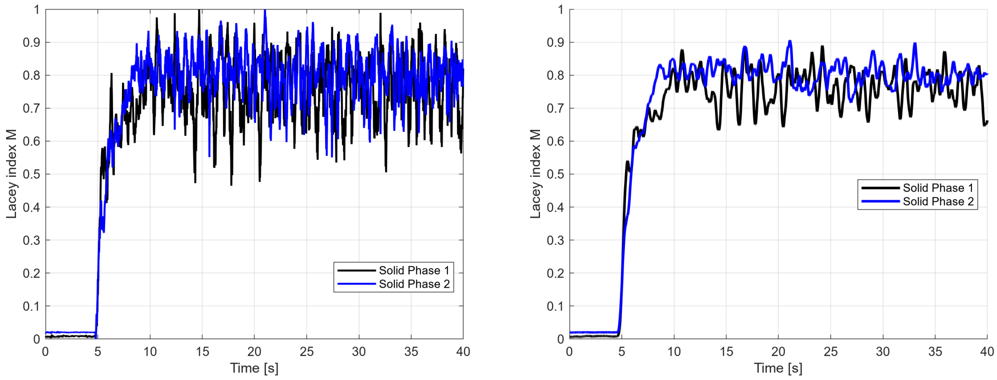

(a) Original temporal evolution of the Lacey indices.

(b) Moving-averaged temporal evolution to reduce fluctuations.

Fig. 4: Temporal evolution of the Lacey mixing indices for the two solid phases segmented from the images. The indices reflect the degree of spatial homogeneity within each phase over time. (a) Original curves showing frame-by-frame values. (b) Smoothed curves obtained by applying a moving average filter to emphasize long-term trends.

The results exhibit two noteworthy behaviors in the computed Lacey indices for the solid phases. First, the indices do not reach the theoretical maximum value of one, even after extended mixing. This suggests that a fully homogeneous spatial distribution is not achieved within the observed timeframe, or that the mixing process maintains some degree of heterogeneity at the analyzed scale. Such submaximal values are consistent with typical physical mixing limitations but may also be influenced by factors related to image processing.

Second, the indices show initial values slightly greater than zero instead of being strictly zero at the start of the mixing process. Ideally, a freshly segregated system would yield an index close to zero, reflecting spatially distinct phases with minimal local mixing. However, this deviation can be partially attributed to artifacts introduced during image segmentation. Noise, partial volume effects, or misclassification of pixels (especially near phase boundaries) can induce spurious local heterogeneities or falsely detected dispersed pixels. These factors artificially increase the measured spatial uniformity, elevating the initial index values.

Therefore, while the Lacey index effectively captures the overall mixing trend, caution is advised when interpreting absolute values. The quality of segmentation and the presence of image artifacts significantly influence the quantitative assessment, and further refinement or validation of the segmentation method may be required to minimize bias in the index calculation.

5 Conclusion

This work has presented a quantitative assessment of the mixing process between two solid phases using the Lacey mixing index computed from segmented image sequences. The segmentation into three classes—background, solid phase 1, and solid phase 2—enabled the independent evaluation of spatial homogeneity evolution for each phase. The temporal analysis of the Lacey indices revealed progressive mixing trends, although the indices did not reach complete homogeneity within the analyzed timeframe.

The study also highlighted the sensitivity of the Lacey index to image processing and segmentation quality. Initial nonzero values of the index emphasize the influence of segmentation artifacts such as noise and pixel misclassification, which can bias the interpretation of mixing degree.

Future work should focus on improving segmentation accuracy and exploring complementary metrics to provide a more robust characterization of mixing dynamics. Additionally, integrating these quantitative image-based indices with physical mixing parameters may enhance the understanding of the underlying mechanisms and support optimization of mixing operations in multiphase systems.

References

[1] Kunii, D., Levenspiel, O.: Fluidization Engineering, 2nd ed. edn. Butterworth-Heinemann, Stoneham, UK (1991)

[2] Garcia-Gutierrez, L.M., Soria-Verdugo, A., Ruiz-Rivas, U.: Optimization of the feeding ports location in a fluidized bed combustor based on monte carlo simulations of fuel particles motion. Fuel **141**, 82–92 (2015)

[3] Rhodes, M.J., Wang, X.S., Nguyen, M., Stewart, P., Liffman, K.: Study of mixing in gas-fluidized beds using a dem model. Chem. Eng. Sci. **56**, 2859–2866 (2001)

[4] Eames, I., Gilbertson, M.A.: Mixing and drift in gas-fluidised beds. Powder Technol. **154**, 185–193 (2005)

[5] Belgardt, D., Schoessler, J., Werther, J.: Lateral non-uniformities of solids and gas concentrations in fluidized bed reactors. In: AIChE Annual Meeting (1986)

[6] Niklasson, F., Thunman, H., Johnsson, F., Leckner, B.: Estimation of solids mixing in a fluidized-bed combustor. Ind. Eng. Chem. Res. **41**, 4663–4673 (2002)

[7] Liu, D., Chen, X.: Lateral solids dispersion coefficient in large-scale fluidized beds. Combust. Flame **157**, 2116–2124 (2010)

[8] Zhang, Y., Jin, B., Zhong, W.: Experiment on particle mixing in flat-bottom spout-fluid bed. Chem. Eng. Process. **48**, 126–134 (2009)

[9] Julián, I., Herguido, J., Menéndez, M.: Particle mixing in a two-section two-zone

fluidized bed reactor. experimental technique and counter-current back-mixing model validation. Ind. Eng. Chem. Res. **52**, 13587–13596 (2013)

[10] Cano-Pleite, E., Hernández-Jiménez, F., Acosta-Iborra, A., Tsuji, T., Müller, C.R.: Segregation of equal-sized particles of different densities in a vertically vibrated fluidized bed. Powder Technol. **316**, 101–110 (2017)

[11] Sánchez-Prieto, J., Hernández-Jiménez, F., Garcia-Gutierrez, L.M., Soria-Verdugo, A.: Experimental study on the characteristic mixing time of solids and its link with the lateral dispersion coefficient in bubbling fluidized beds. Chemical Engineering Journal **307**, 113–121 (2017)

[12] Bokkers, G.A., Sint Annaland, M., Kuipers, J.A.M.: Mixing and segregation in a bidisperse gas-solid fluidized bed: a numerical and experimental study. Powder Technol. **140**, 176–186 (2004)

[13] Kuipers, J.A.M., Van Duin, K.J., Van Beckum, F.P.H., Van Swaaij, W.P.M.: A numerical model of gas-fluidized beds. Chemical Engineering Science **47**(8), 1913–1924 (1992)

[14] Gidaspow, D.: Multiphase flow and fluidization: Continuum and kinetic theory descripctions. Academic Press, San Diego, CA (1994)

[15] Hernández-Jiménez, F., Sánchez-Prieto, J., Cano-Pleite, E., Soria-Verdugo, A.: Lateral solids meso-mixing in pseudo-2d fluidized beds by means of tfm simulations. Powder Technology **334**, 183–191 (2018)

[16] Deen, N.G., Sint Annaland, M., Hoef, M.A., Kuipers, J.A.M.: Review of discrete particle modelling of fluidized beds. Chem. Eng. Sci. **62**, 28–44 (2007)

[17] Müller, C.R., Holland, D.J., Sederman, A.J., Scott, S.A., Dennis, J.S., Gladden, L.F.: Granular temperature: comparison of magnetic resonance measurements with discrete element model simulations. Powder Technol. **203**, 241–253 (2008)

[18] Hernández-Jiménez, F., Third, J.R., Acosta-Iborra, A., Müller, C.R.: Comparison of bubble eruption models with two-fluid simulations in a 2d gas-fluidized bed. Chem. Eng. J. **171**, 328–339 (2011)

[19] Müller, C.R., Davidson, J.F., Dennis, J.S., Hayhurst, A.N.: A study of the motion and eruption of a bubble at the surface of a two-dimensional fluidized bed using particle image velocimetry (piv). Ind. Eng. Chem. Res. **46**, 1642–1652 (2007)

[20] Lacey, P.M.C.: Developments in the theory of particle mixing. Journal of Applied Chemistry **4**(4), 257–268 (1954)

[21] Hull, A.S., Chen, Z., Agarwal, P.K.: Influence of horizontal tube banks on the behavior of bubbling fluidized beds: 2. mixing of solids. Powder Technol. **111**,

192–199 (2000)

[22] Gorji-Kandi, S., Alavi-Amleshi, S.M., Mostoufi, N.: A solids mixing rate correlation for small scale fluidized beds. Particuology **21**, 55–64 (2015)

[23] Julián, I., Herguido, J., Menéndez, M.: Experimental and simulated solids mixing and bubbling behavior in a scaled two-section two-zone fluidized bed reactor. Chem. Eng. Sci. **143**, 240–255 (2016)

[24] Sánchez-Prieto, J., Soria-Verdugo, A., Briongos, J.V., Santana, D.: The effect of temperature on the distributor design in bubbling fluidized beds. Powder Technol. **261**, 176–184 (2014)

[25] Gonzalez, R.C., Woods, R.E.: Digital Image Processing, 2nd edn. Prentice Hall, Upper Saddle River, NJ, USA (2002)